Progress in Organic Coatings 167 (2022) 106825

Contents lists available at ScienceDirect

Progress in Organic Coatings

journal homepage: www.elsevier.com/locate/porgcoat

Thermal and mechanical properties of thiol-ene photocured thermosets containing DOPO-based liquid reactive flame retardant synthesized by metal-free azide-alkyne click reaction

Gokhan Sagdic [a], Emrah Cakmakci [b,*], Ozgun Daglar [a], Ufuk Saim Gunay [a,*], Gurkan Hizal [a], Umit Tunca [a], Hakan Durmaz [a]

[a] Department of Chemistry, Istanbul Technical University, 34469 Istanbul, Turkey
[b] Department of Chemistry, Marmara University, 34722 Istanbul, Turkey

ARTICLE INFO

Keywords:
Thiol-ene photopolymerization
Metal-free click reaction
Flame retardant
DOPO
Synergism

ABSTRACT

The use of metal-free click reactions for the design and synthesis of novel flame retardant reactive monomers for thiol-ene photopolymerization is an intriguing area of research. In this study, we have prepared a new, 9,10-dihydro-9-oxa-10-phosphaphenanthrene-10-oxide (DOPO)-based, P- and N-containing reactive flame retardant via the metal-free azide-alkyne click reaction. For this purpose, first, azide-functionalized DOPO (DOPO-N_3) has been synthesized via Atherton–Todd reaction, and then this compound has been reacted with acetylene dicarboxylic acid diallyl ester (ACDAE) to give the flame retardant monomer, namely DOPO-triazole diallyl ester (DTDAE). As prepared flame retardant monomer was characterized by nuclear magnetic resonance (NMR) and Fourier-transform infrared spectroscopy (FTIR) spectroscopies. Thermoset materials prepared by using DTDAE displayed over 90% gel content values. Polar triazole and phosphorous units rendered the surface of the thermosets hydrophilic. The thermal stability of the networks was enhanced, char yields increased and the glass transition temperatures (T_gs) were increased. The limiting oxygen index (LOI) values of the crosslinked materials increased up to 27.8% as the DTDAE content was increased in the formulations. The synthetic method described in this study provides a practical approach for the synthesis of a P- and N-containing flame retardant through a metal-free azide-alkyne click reaction Also, the fact that DTDAE is in a liquid state makes this study valuable as it indicates that it can be easily dispersed. It is also believed this promising compound can be used in different polymer structures and formulations to develop new flame retardants in future studies to be applied in industrial applications.

1. Introduction

Every year fires cause the death of thousands of people and billions of dollars in economic losses. According to National Fire Protection Association (NFPA), 1.4 million fires occurred in the USA alone, resulting in 3500 civilian deaths, 15,200 civilian injuries and accounting for a $21.9 billion estimated property damage. 26% of these fires occurred in houses yet they caused 74% of the civilian deaths [1]. Considering this high ratio of house fires related deaths, the importance of fire retardant monomers, polymers, or agents used in home textiles, furniture, beddings, carpets, curtains, coatings, etc., can be understood.

Thiol-ene photopolymerization (TEP) is a modern technique within the tool kit of polymer chemists and also a superior alternative to classical photopolymerization techniques. According to the mechanism of TEP, multifunctional thiol compounds generate thiyl radicals upon light irradiation even in the absence of a photoinitiator (or thiyl radicals are generated by proton abstraction by the radicals formed by the cleavage of photoinitiators) and then these thiyl radicals quickly add to the multifunctional double bond-containing monomers to give crosslinked networks [2–4]. Thus, TEP is known to follow a radical-mediated step-growth mechanism [5]. TEP offers unique properties such as resistance to oxygen inhibition, fast curing rates, spatial control over polymerization, homogeneous network structures, modularity, low shrinkage, high monomer conversion percentages, tunability, stereoselectivity, photoinitiator-free curing, etc. [2–8]. Besides, a large pool of –ene species including those that do not undergo homopolymerization

* Corresponding authors.
E-mail addresses: emrah.cakmakci@marmara.edu.tr (E. Cakmakci), gunayuf@itu.edu.tr (U.S. Gunay).

https://doi.org/10.1016/j.porgcoat.2022.106825
Received 12 January 2022; Received in revised form 28 February 2022; Accepted 9 March 2022
Available online 17 March 2022

can react via thiol-ene reactions. Due to the versatile and robust characteristics, thiol-ene reactions are regarded as click reactions and these exceptional features render TEP suitable for a wide range of applications including coatings, optical and biomedical devices, high-resolution lithography, polymer, and surface functionalization, electro-optics, nanoimprinting, and liquid crystal, and holographic materials, etc. [9]. Nevertheless, some drawbacks like poor mechanical properties, low T_gs, odor, and flammability accompany these advantageous features.

In recent years, many studies have been devoted to the improvement of the mechanical and thermal properties of the TEP-based networks [10–14]. Among these works, the synthesis of flame retardant monomers for TEP has become an active area of research. In our previous work, we successfully applied three different metal-free click reactions: azide-alkyne cycloaddition, thiol- and aza-Michael addition reactions, on acetylene dicarboxylic acid diallyl ester (ACDAE) [14]. The resulting phosphorous, nitrogen, and fluorine-containing monomers were then used to form thiol-ene photocured networks, but the gel contents and the flame retarding performance of the resulting networks in that work were found to be relatively low. We reasoned that the low gel contents resulted from the strong light absorption of those monomers between 300 and 360 nm which overlapped with the absorption of the photoinitiators and the relatively poor flame retardancy was attributed to the low amount of phosphorous in the synthesized monomers.

The ease of metal-free functionalization of ACDAE stems from its electron-deficient alkyne group which facilitates the aforementioned click reactions to occur efficiently. Previously several polymers with a wide range of features were prepared by using various acetylene dicarboxylic acid derivatives [15–25]. Since the flame retardancy of the networks was relatively low in our previous work, in this study we designed another novel flame retardant monomer with a higher phosphorus (P) percentage. The new monomer, namely DOPO-triazole diallyl ester (DTDAE) was prepared via a metal-free azide-alkyne click reaction between ACDAE and an azide-functionalized DOPO (DOPO-N_3). In this study, DOPO is purposely selected since it has been a widely used flame retardant compound that leads to higher thermal stability than other phosphorus units [26]. Here, we modified DOPO with triazole units and reactive groups to prepare flame retardant thermoset materials. The efficiency of triazole-containing flame retardants was investigated in previous studies [27–30]. The monomer, DTDAE, was characterized by using NMR and FTIR spectroscopies and used for the preparation of thiol-ene photocured thermosets. The mechanical, thermal, optical, and flame retardant properties of the crosslinked networks were determined.

2. Experimental

2.1. Materials

Pentaerythritoltetrakis(3-mercaptopropionate) (4SH), diallyl phthalate (DAP), sodium azide, methanol, anhydrous sodium sulfate, triethylamine (Et_3N), 2-bromoethanol, *p*-toluenesulfonic acid monohydrate, benzene, hexane, sodium chloride, dichloromethane (DCM), chloroform ($CHCl_3$), carbon tetrachloride (CCl_4), and 2-methyltetrahydrofuran (2-MeTHF) were all purchased from Sigma Aldrich and used as received. 2,4,6-Trimethylbenzoyl-diphenyl-phosphineoxide (TPO) and 2-hydroxy-2-methyl-1-phenyl-1-propanone (Darocur 1173) were obtained from Ciba Specialty Chemicals. 9,10-dihydro-9-oxy-10-phosphaphenanthrene-10-oxide (DOPO) was obtained as a gift from MCTCHEM (Turkey). 2-Azidoethanol and acetylene dicarboxylic acid diallyl ester (ACDAE) were synthesized according to our previously published procedures [14].

2.2. Characterization

FTIR spectra were recorded on a Cary 630 FTIR (Agilent Technologies) instrument over the range 4000–600 cm^{-1}. ^1H (500 MHz), ^{13}C (125 MHz) were recorded using an Agilent VNMRS 500 instrument in $CDCl_3$ and ^{31}P NMR (162 MHz) spectra were recorded using a Varian 400 instrument in $CDCl_3$. Differential scanning calorimetry (DSC) experiments were performed under a nitrogen atmosphere on the PerkinElmer Pyris Diamond DSC apparatus. Thermogravimetric analyses (TGA) of the photocured films were performed by using a PerkinElmer thermogravimetric analyzer (Pyris 1 TGA model). Samples were run from 30 to 600 °C with a heating rate of 10 °C/min under a nitrogen atmosphere. The water contact angles (CA) of the coatings were determined on a Kruss (Easy Drop DSA-2) tensiometer. Measurements were made using 3–5 μL drops of distilled water. For each sample, at least three measurements were made, and the average was taken. The transmission spectra of the coatings were obtained by using a Shimadzu 3100 UV–vis-NIR spectrometer. Gel contents of the coatings were determined by soxhlet extraction of the pre-weighted films for 24 h with $CHCl_3$. Insoluble gel fraction was dried in a vacuum oven at 40 °C to constant weight and the gel percentage was calculated. LOI values of the thermosets were measured by using a FTT (Fire Testing Technology) type instrument, according to ASTM D2863–08. The test specimen bars of 120 × 6 × 3 mm^3 were prepared for the LOI test. UL-94 vertical burning test was conducted according to ASTM D3801 by using test specimens in 120 × 13 × 3 mm^3. Mechanical properties of the thermosets were determined at room temperature on a Materials Testing Machine Z010 / TN2S. The polymerization conversion was followed by real-time infrared spectroscopy. The details of the measurement and calculations were described elsewhere [14].

2.3. Synthesis of 6-(2-azidoethoxy)dibenzo[c,e][1,2]oxaphosphinine 6-oxide (DOPO-N_3)

DOPO-N_3 was prepared using the similar conditions described in previous examples [31,32]. Briefly, into a 100 mL round bottom flask, DOPO (4.32 g, 20.0 mmol), DCM (20 mL), and Et_3N (3.07 mL, 22.0 mmol) were added in that order while stirring. Upon complete dissolution of DOPO, 2-azidoethanol (1.92 g, 22.0 mmol) was added to the reaction mixture, then the mixture was cooled to 0 °C in an ice bath. After that, CCl_4 (2.13 mL, 22.0 mmol) was added to the reaction medium dropwise, then the flask was removed from the ice bath and left to stir overnight at room temperature. The mixture was diluted with 50 mL of DCM and extracted with 100 mL of distilled water three times. The organic layers were dried over Na_2SO_4, filtered, and evaporated to dryness to give DOPO-N_3 as a pale yellow liquid. Yield: 4.47 g, 74%. ^1H NMR ($CDCl_3$, δ) 7.95–7.27 (m, 8H, Ar—H), 4.31 (m, 2H, P=OOCH_2CH_2N$_3$), 3.43 (t, 2H, P=OOCH$_2$CH_2N$_3$). ^{13}C NMR ($CDCl_3$, δ) 149.69, 137.08, 133.78, 130.60, 130.29, 128.42, 125.31, 124.90, 124.07, 122.40, 120.89, 120.18, 64.83, 50.95. ^{31}P NMR ($CDCl_3$, δ) 10.89.

2.4. Synthesis of diallyl 1-(2-((6-oxidodibenzo[c,e][1,2]oxaphosphinin-6-yl)oxy)ethyl)-1H-1,2,3-triazole-4,5-dicarboxylate (DTDAE)

To a 25 mL Schlenk tube was added DOPO-N_3 (2.00 g, 6.64 mmol) and ACDAE (1.42 g, 7.31 mmol) equipped with a magnetic stir bar and dissolved in 7 mL of 2-MeTHF. After 2 freeze-pump-thaw cycles, the tube was placed in an oil bath at 80 °C for 24 h. Afterward, the solution was precipitated into 70 mL of hexane, then the excess solvent was removed by decantation and the pale yellow oil was recovered. The obtained crude product was further purified by a second dissolution–precipitation ($CHCl_3$-hexane) procedure. Finally, the precipitate was dried in vacuo for 24 h to give DTDAE as a pale yellow viscous transparent oil. Yield: 3.20 g, 97%. ^1H NMR ($CDCl_3$, δ): 7.87–7.14 (m, 8H, Ar—*H*), 6.04–5.82 (m, 2H, OCH$_2$C*H*=CH$_2$), 5.46–5.28 (m, 4H, OCH$_2$CH=CH_2), 4.84 (m, 4H, C═OOCH_2), 4.66–4.50 (m, 4H, P=OOCH_2CH_2N$_3$-triazole). ^{13}C NMR ($CDCl_3$, δ) 159.46, 157.80, 149.37, 139.85, 137.13, 133.88, 131.36, 130.71, 130.14, 128.31, 125.28, 124.91, 124.08, 122.14, 121.63, 119.98, 119.92, 119.45, 67.23, 66.39, 63.61, 50.04. ^{31}P NMR

($CDCl_3$, δ) 10.90.

The synthesis of DTDAE is illustrated in Scheme 1.

2.5. Preparation of thiol-ene photocurable formulations

Required amounts (Table 1) of DAP and DTDAE were weighed into a clean beaker wrapped with aluminum foil to prevent pre-polymerization. The mixture in the beaker was stirred at 60 °C for 10–15 min until homogenization. Next, TPO was added to this mixture and stirred at 60 °C until it was dissolved. Finally, the mixture was cooled to room temperature and 4SH and Darocur 1173 were added. The homogeneous mixtures were degassed in a vacuum oven. The mixtures were then poured into Teflon molds and cured under UV irradiation (OSRAM, 300 W, λ_{max} = 365 nm, 10 mW/cm^2) for 10 min with 1-min intervals. The preparation of the photocured networks is depicted in Scheme 2. Formulations were encoded as DTFRX where, D, T, and FR represents, DAP, 4SH, and DTDAE, respectively, and X represents the approximate weight ratio of the DTDAE in the formulations.

Table 1
Thiol-ene photocurable formulations[a].

Code	DAP (mol)	4SH (mol)	DTDAE (mol)	DTDAE %	P and N (%)	Gel content (%)
DTFR0	0.01	0.005	0	0	0	98
DTFR10	0.009	0.005	0.001	9.32	0.6 and 0.82	94
DTFR20	0.008	0.005	0.002	17.84	1.16 and 1.57	93
DTFR30	0.006	0.005	0.004	32.83	2.13 and 2.89	91
DTFR45	0.004	0.005	0.006	45.61	2.96 and 4.01	92
TFR65	0	0.005	0.01	66.23	4.30 and 5.82	93

[a] 1% TPO and 3% Darocur 1173 were added to each formulation.

3. Results and discussion

3.1. Characterization of DTDAE

The azide-functionalized DOPO (DOPO-N_3) was prepared by

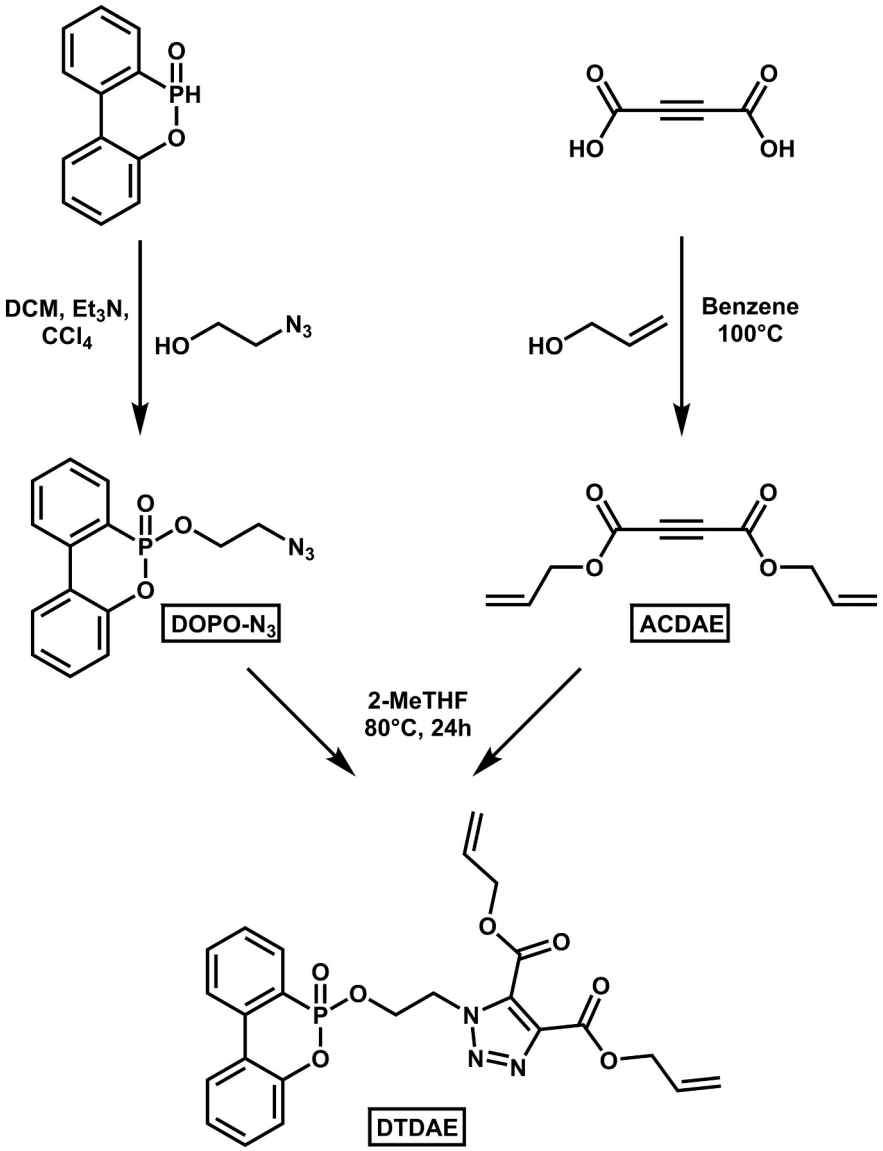

Scheme 1. Synthetic route for the preparation of DTDAE.

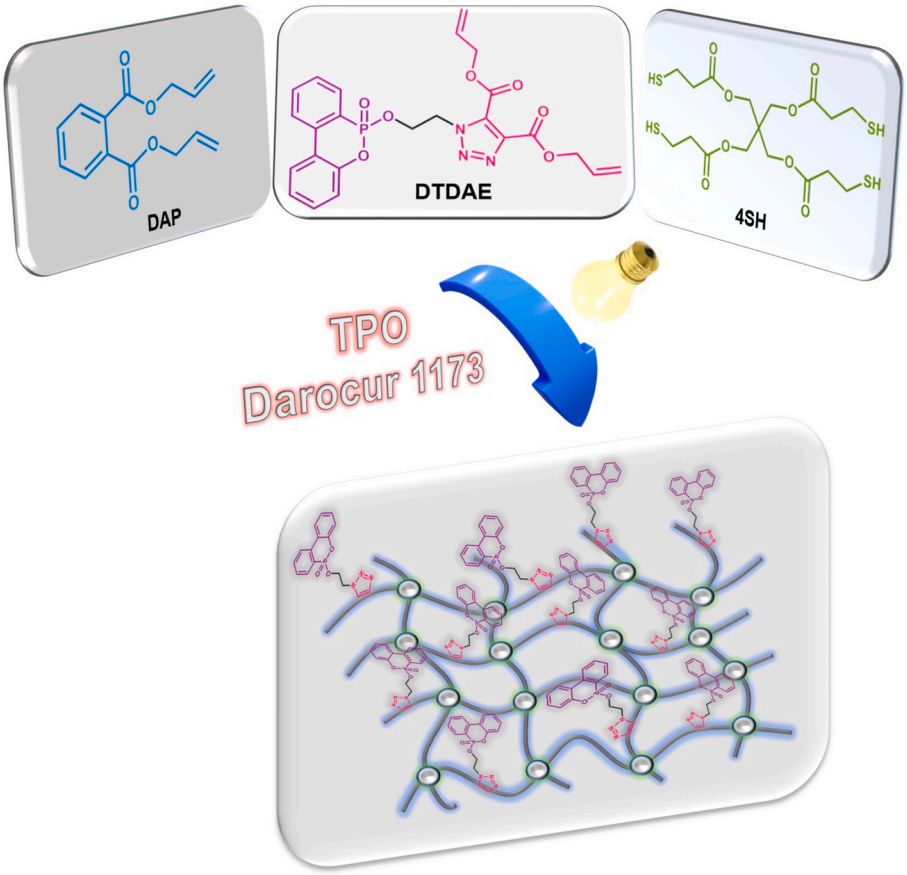

Scheme 2. The schematic representation of the formation of flame retardant thiol-ene photocured thermosets.

Atherton–Todd reaction, which was previously noted in the literature as a useful tool for the preparation of flame retardant materials [31,32]. Then, DTDAE was synthesized from the reaction of ACDAE with DOPO-N_3 by using a metal-free azide-alkyne click reaction. The DOPO-N_3 and DTDAE were characterized via NMR spectroscopy (Fig. 1).

The aromatic protons of DOPO were resonated between 8.0 and 7.0 ppm. In addition to the aromatic protons, two methylene signals corresponding to the P=OOCH_2CH_2N$_3$ unit were observed at 4.3 ppm and 3.4 ppm, confirming the structure of DOPO-N_3. After the metal-free azide-alkyne click reaction, these protons were slightly shifted downfield and appeared at 4.66–4.50 ppm. Moreover, the allylic protons were observed between 6.0 and 5.0 ppm. The signal at 4.38 ppm corresponds to the methylene protons adjacent to the ester oxygen. Also, the ^{31}P NMR spectra of the aforementioned compounds embedded in Fig. 1 exhibited clear single peaks at 10.90 ppm regarding the phosphorus atom of the *P*=O unit, indicating that the synthesized monomers are pure. Meanwhile, the ^{13}C NMR spectra confirming the successful preparation of these compounds are given in Figs. S1 and S2.

DTDAE was further characterized by FTIR spectroscopy (Fig. S3). The band at 1720 cm^{-1} belongs to the characteristic ester carbonyl groups while the band at 1648 cm^{-1} is due to the allyl double bond stretching vibrations. The strong band at 918 cm^{-1} was attributed to the P–O-Ph group of DOPO [33]. The absence of an azide stretching vibration band at around 2100 cm^{-1} also proves that the click reaction was successful and the monomer is pure. Furthermore, the UV–Vis spectrum of DTDAE was recorded (Fig. S4). It was found that DTDAE does not absorb light until 300 nm and has maximum absorption (λ_{max}) at 297 nm. This wavelength of the absorption maximum is lower than the values we obtained in our previous work [14].

3.2. Structural characterization of the photocured thermosets

The thermosets were structurally characterized by FTIR spectroscopy while the extent of curing was investigated by measuring the gel content values and real-time infrared spectroscopy. The FTIR spectra of the liquid formulations displayed the characteristic vibration bands of all the monomers within (Fig. 2). The -SH groups were observed as weak bands at 2577 cm^{-1}. The allyl bands were also detected at 1648 cm^{-1}. In all spectra, bands were observed at around 1600 cm^{-1} which correspond to the –C=C- bonds in the aromatic rings in DAP and DTDAE. After UV-induced polymerization, the allyl and thiol vibration bands were completely disappeared, indicating that the formulations were thoroughly cured.

Gel content is a crucial parameter that shows the degree of curing. The gel contents of the thermosets were found to be over 90% (Table 1). The gel content of the DTDAE-free formulation was measured as 98%, it decreased to 94% when 10% DTDAE was introduced. With further DTDAE addition, gel content values decreased to 91%.

To further evaluate the extent of curing real-time spectroscopy was used and the conversion of the allyl groups was monitored. We could not be able to monitor the conversion of the thiol groups due to their relatively low intensities. According to the allyl conversion plots (Fig. 3), it can be said that in all cases, owing to the thiol-ene mechanism, very fast conversion rates were achieved. Almost within 10 s over 90% of the allyl groups were reacted. A slight and gradual decline was observed in the allyl conversions as the amount of DTDAE was increased. In a previous study where a similar system was investigated, the allyl conversion profile of the crosslinked networks composed of diallyl terephthalate (DATP) and pentaerythritol tetrakis(3-mercaptobutyrate), was found to be identical to this work [34].

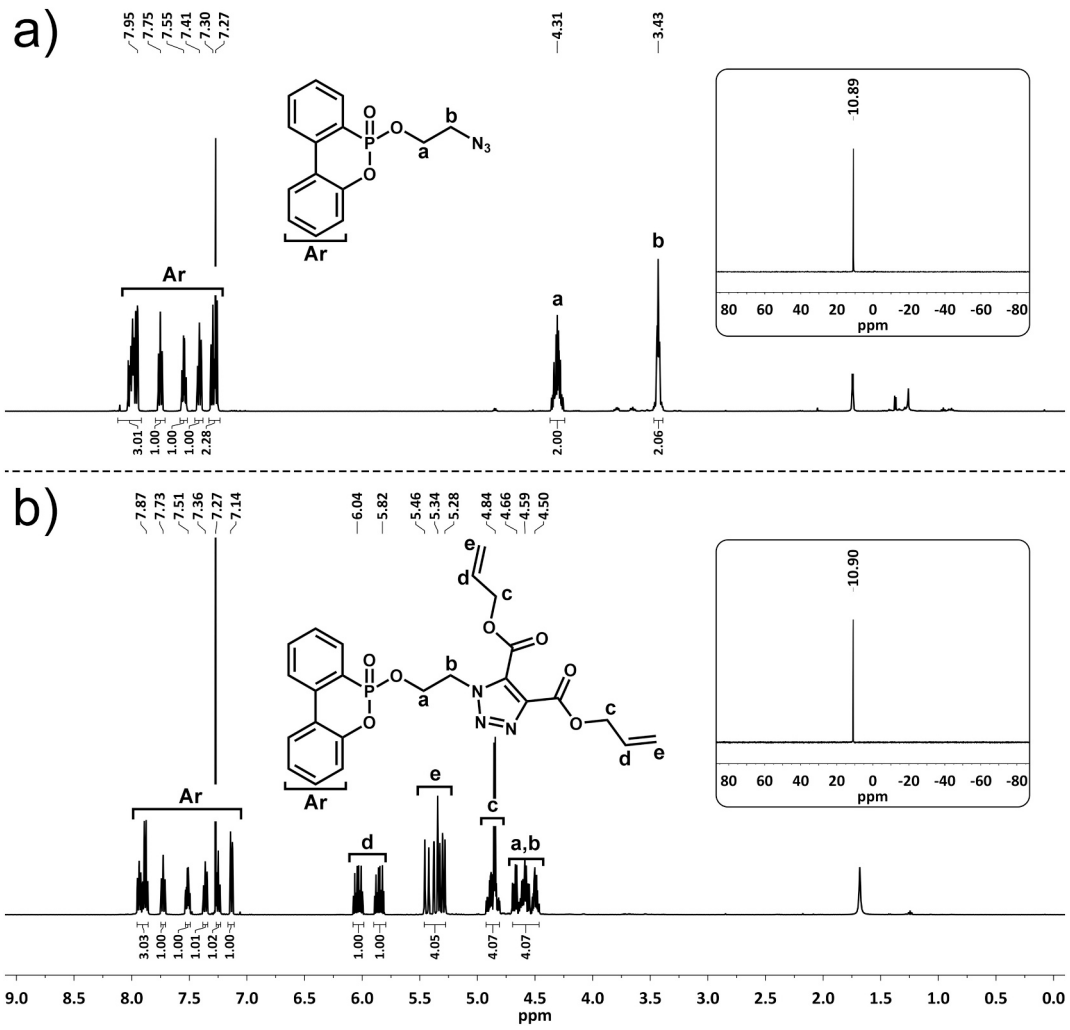

Fig. 1. ^{1}H and ^{31}P NMR (embedded to ^{1}H NMR) spectra of DOPO-N_3 and DTDAE in $CDCl_3$.

3.3. Wettability of the photocured networks

The WCA values of the thermosets were determined (Fig. 4) to assess the effect of DTDAE on the wettability of the photo-crosslinked networks. The water contact angles (CA) of the thermosets were determined on a tensiometer. A drop of distilled water (3-5 μL) was carefully placed on the surface of the films with the aid of a syringe. Next, with the aid of the software of the instrument (Krüss) the photographs of the films with the water drop on them were recorded and the contact angles were measured. For each sample, at least three measurements were made, and the average was taken. While DTFR0 displayed a WCA of 72, the WCA values of the DTDAE-containing networks decreased gradually. A slight increase in the WCA values was observed for DTFR45 and TFR65 encoded samples but still, the surfaces of the DTDAE-containing thermosets were found to be hydrophilic with respect to the DTFR0. The reason for the increased hydrophilicity can be attributed to the introduction of polar triazole rings and phosphorous units [14].

3.4. Optical properties

The optical light transmittance of the thermosets with respect to the wavelength is an important feature for some applications that require transparent materials. The transmittance percentages of the thermosets were determined between 300 and 800 nm (Fig. S5) and the thickness of the thermosets was about 1 mm for all samples. The transmission percentages of all samples were above 90% between 600 and 800 nm. As the wavelength shifted toward the UV region, the transmittance of the thermosets decreased significantly as a result of the strong UV absorption of DAP as well as the DTDAE. When the transmittance values of the DTDAE-containing networks were compared to the transmittance of the base formulation, it can be said that DTDAE's contribution to UV absorption is much more pronounced.

3.5. Mechanical properties

One of the main problems associated with the use of flame retardant monomers is that even if they outperform in terms of flame retardancy, they can adversely affect the mechanical properties. Unfortunately, the mechanical properties were also reduced in this study when DTDAE was added (Table 2 and Fig. 5). Note that the values given in Table 2 are average results of at least three different measurements. The Young modulus (E) of the base formulation; DTFR0 was determined as 6.12 MPa. The modulus decreased gradually with increasing amount DTDAE up to 30% then slightly increased when its percentage was reached 45%. On the other hand, after a slight decrease in the tensile strength with the incorporation of DTDAE to the base formulation, tensile strengths did not change drastically. The elongation at break values also declined with the addition of DTDAE, however, when the DTDAE's concentration was reached 30%, a remarkable increase was observed in the elongation values. This high elongation at break value was also observed for DTFR45 encoded thermosets. When DAP was completely replaced with DTDAE, the tensile strength and the elongation at break values were

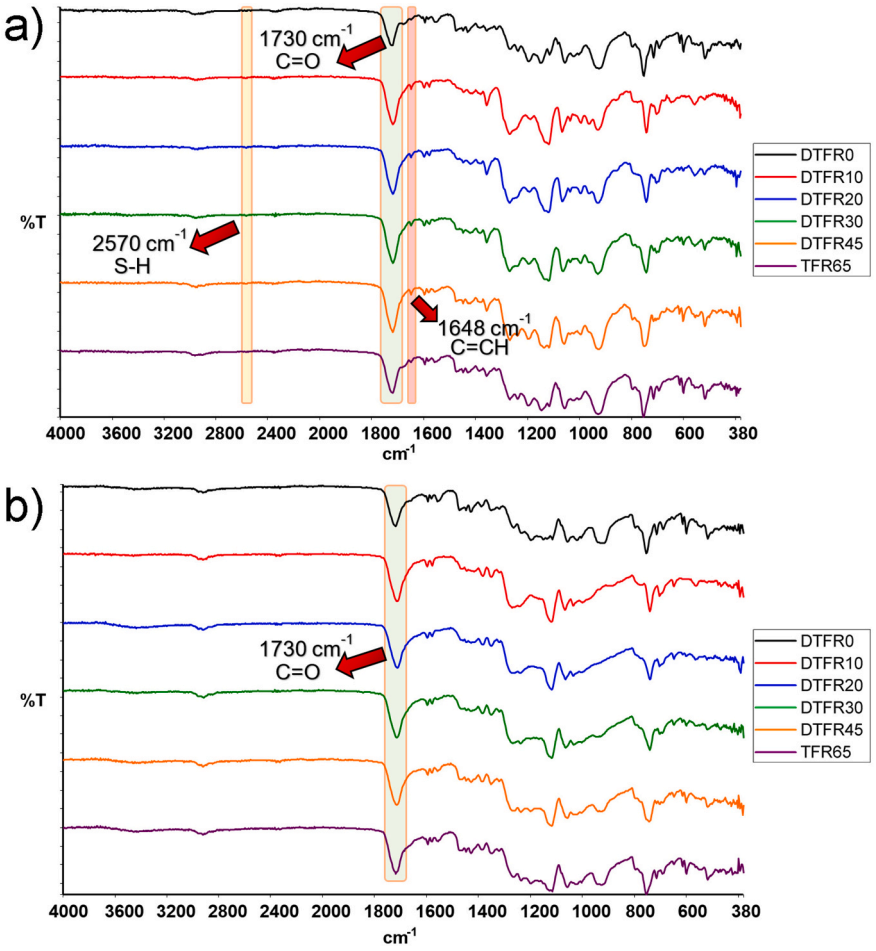

Fig. 2. FTIR spectra of the liquid precursors (a) and the cured thermosets (b).

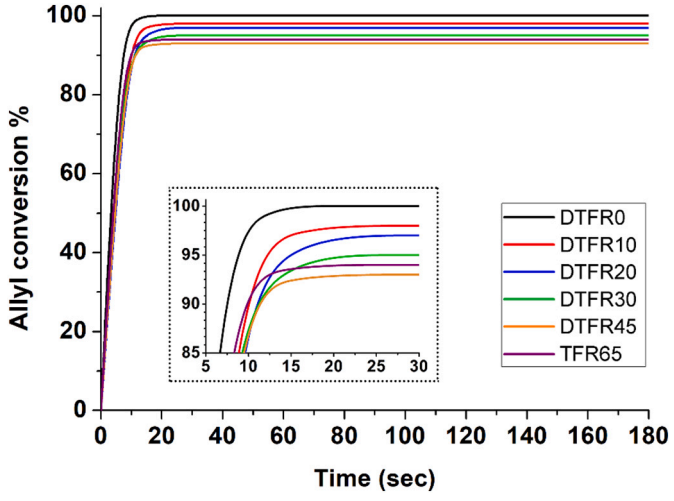

Fig. 3. Double bond conversion percentages of the photocurable formulations. The inset shows an expanded section of the spectrum.

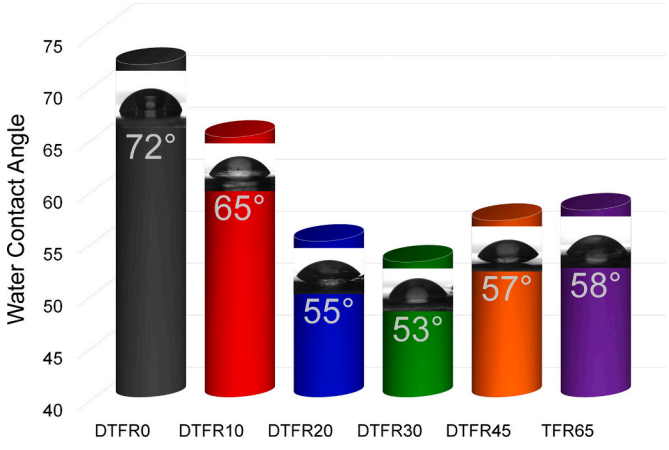

Fig. 4. WCA values of the photocured films.

found to be comparable to the base formulation but the E value of the TFR65 was lower than the DTFR.

Here, the declined mechanical properties can be attributed to the decreased crosslinking density of the thermosets which is evident from both the gel content values and the allyl conversion percentages. Mongkhontreerat et al. prepared several thiol-ene photocured rigid, soft, or hydrogel networks by using various –enes and thiols in different thiol to -ene ratios, and in some formulations, when excess thiols were used, a dramatic decrease in the modulus values were observed [35]. For instance, Young's modulus value decreased to 106 kPa from 782 MPa when -ene to thiol ratio was changed to 1:2.5 from 1:1 or it decreased to 615 MPa when a 1.5:1 ene to thiol ratio was employed as a result of the decreased crosslinking density.

Table 2
Thermal and mechanical properties of the photocured resins.

	Modulus (MPa)	Tensile Strength (MPa)	Elongation at break (%)	T_1[a] (°C)	T_2[a]	Char (%)	T_g[b] (°C)	LOI	UL-94[c] rating
DTFR0	6.12	1.23	32	356	430	5.6	4.4	20.8	NR
DTFR10	5.51	0.96	17	355	440	6.7	7.6	22.4	NR
DTFR20	2.96	0.93	17.6	351	430	8.2	12.0	23.2	NR
DTFR30	1.83	–	83	352	420	12.0	13.0	24.6	NR
DTFR45	2.09	–	86	310/350	550	11.2	13.2	25.4	V-1
TFR65	1.77	1.10	32	310/350	520	12.2	16.0	27.8	V-0

[a] T_1 and T_2 are the maximum weight loss temperatures, which were determined from the maximum of the corresponding derivative curves.
[b] Determined by DSC.
[c] NR: not rated.

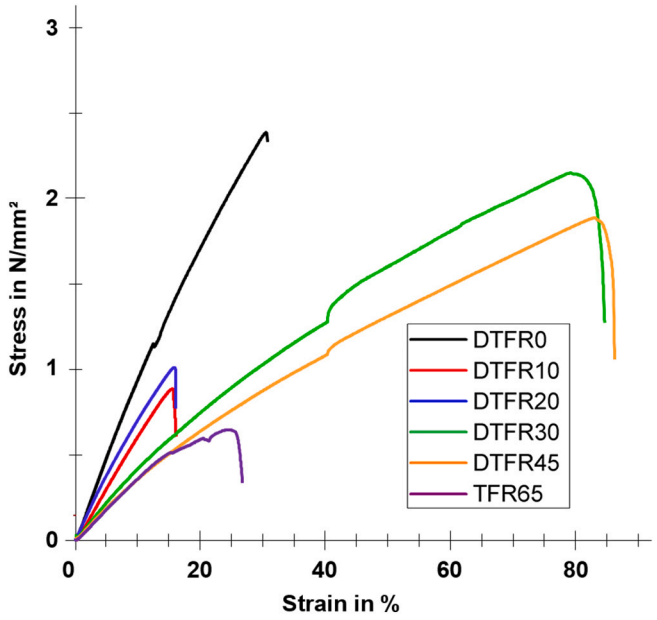

Fig. 5. Representative stress-strain curve of the photocured films.

3.6. Thermal properties and flame retardancy of the cured thermosets

The thermal degradation profiles of the photocured thermosets were determined employing TGA. The TGA spectra and the derivative weight curves are presented in Fig. 6. The results of the TGA are also collected in Table 2.

Mainly, the thermosets displayed a two-step degradation process. The first maximum degradation step was around 350 °C and it was attributed to the degradation of the aliphatic groups of the crosslinked chains while the second maximum degradation was attributed to the decomposition of the aromatic groups. As the amount of DTDAE was increased in the formulations, an additional degradation step which is much more significant in DTFR45 and TFR65 was observed at around 310 °C. This was attributed to the degradation of the phosphorous groups which was encountered many times in the literature [36–38]. For the other thermosets which contain relatively less DTDAE, this step was not very clear but a slight reduction of the first maximum weight loss temperatures was observed. Besides, the second maximum degradation temperatures were improved remarkably with the addition of DTDAE and when its amount was 45%, over a hundred degrees of increase in the second weight loss temperature was detected concerning the base formulation. The char yields increased gradually with the increasing amount of DTDAE and reached over 12% when DAP is completely replaced with DTDAE. The high char yields are generally associated with the flame retardancy of polymers. Thus, it can be said that the flame retardancy of the DTDAE-containing thermosets was improved. We further evaluated the flame retardancy of the thermosets by the LOI test in which the minimum amount of oxygen that is needed to support flaming combustion is measured.

The LOI values of the thermosets are plotted in Fig. 7. The inlay images in this plot display the digital photographs of the films and the formed char mass for TFR65. The DTFR0 encoded sample had a LOI value of 20.8. In a previous work, DAP and 4SH were polymerized with 1,3,5-triallyl-1,3,5-triazine-2,4,6(1H,3H, 5H)-trione (TTT) and the LOI value of this composition was found as 21.6% [10]. The presence of nitrogen due to TTT might be responsible for this relatively higher LOI value. As DTDAE was increased in the thermoset films, the LOI values increased significantly. DTFR45 which contains almost 3% P and 4% N, displayed a LOI value of 25.4. With the elimination of DAP from the thermosets, the amount of P and N were further increased in TFR45 and the LOI value was measured as 27.8%. These high LOI values do not only stem from the high P percentages in the formulations but also arise due to P and N synergism. This effect is reflected in the formed dense char (see the encircled image in Fig. 7).

Furthermore, the flame retardant performance of the thiol-ene photocured thermosets was evaluated by measuring their UL-94 ratings. In each case, the cotton was not ignited. The total afterflame times (t_1 and t_2) for DTFR0, DTFR10, DTFR20, and DTFR30 were found to be over 250 s. Thus, they were not rated according to the UL-94 test (see Table 2). On the other hand, the DTFR45 and TFR65 were rated as V-1 and V-0, respectively. Ai et al. synthesized phosphorous and triazole-containing flame retardant, added it to epoxy thermosets and even though as high as 32.5% LOI value was achieved, none of the thermosets passed the UL-94 test [28]. Owing to the high amount of phosphorous in this work, a V-0 rating was reached for the fully DTDAE-containing sample.

P-containing flame retardant agents act both in the gas and condensed phase [39]. According to the mechanistic studies for the flame retardant action of P- and triazole-containing flame retardants, triazole units release nitrogen-containing gases such as N_2 and NH_3 and dilute the oxygen and heat in the gas phase along with the P-containing radicals which entrap active free-radicals [28–30]. In the condensed phase, P-containing units generate species like phosphoric acid upon decomposition and these species catalyze the carbonaceous char formation. Volatiles such as N_2 and NH_3 expand the residue and lead to swollen foam-like char. Eventually, the intumescent char impedes the transfer of heat and oxygen to the underlying coating, thereby enhancing the overall thermal stability and flame retardancy. Furthermore, especially for a DOPO- and triazole-based flame retardant, TG–FTIR, and pyrolysis–gas chromatography/mass spectrometer (Py–GC/MS) studies identified the presence of species like biphenyl, *o*-hydroxybiphenyl, *o*-aminobiphenyl, 4-methyl-dibenzofuran, and carbazole, etc., in the gas phase, originating from DOPO [27].

In our case, even though the intumescent behavior was not profound, foamed char formation was evident and thus, DTDAE can be described as an effective intumescent flame retardant reactive monomer. Finally, it can be concluded that thermal properties and flame retardancy of the thermosets were improved owing to the synergism between DOPO units

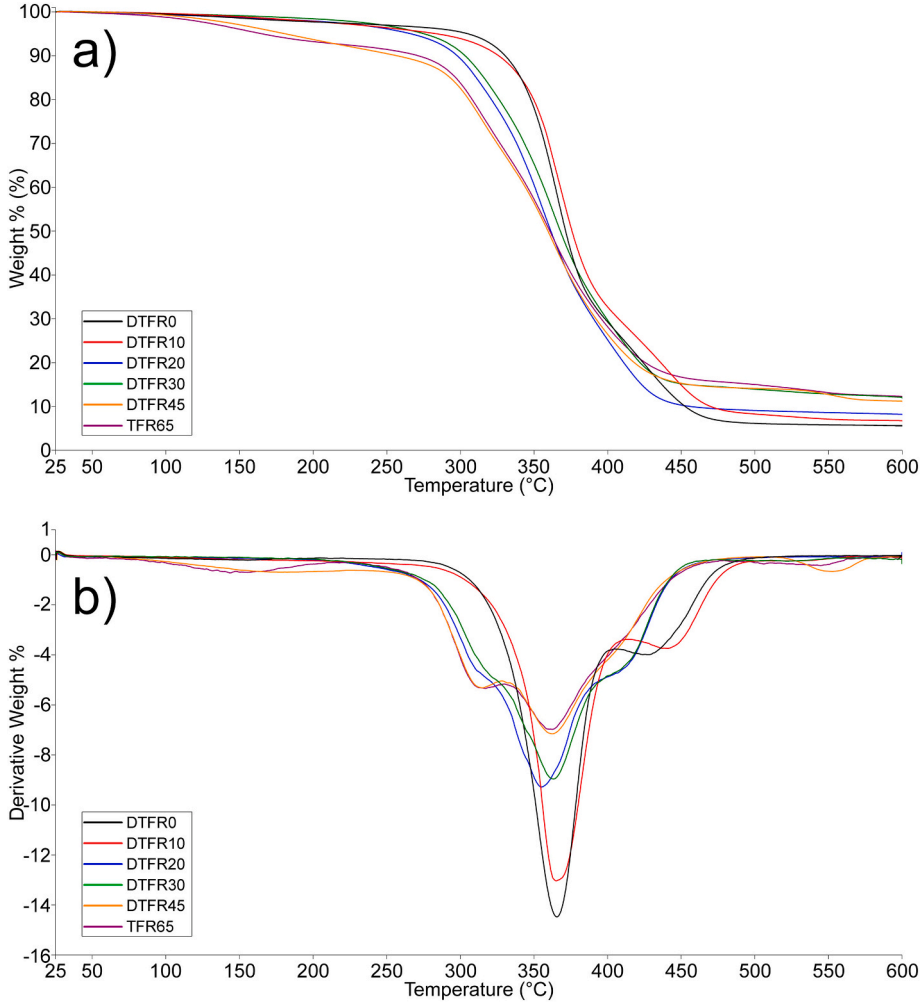

Fig. 6. TGA thermograms (a) and the derivative weight curves of the photocured thermosets (b).

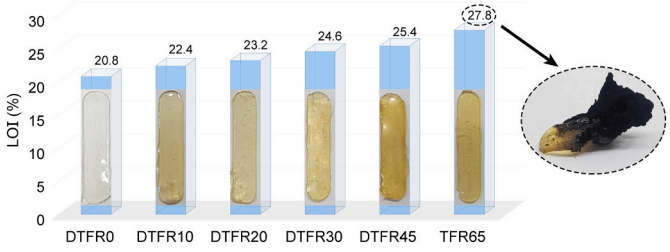

Fig. 7. LOI values of the thermosets. The images on the columns are the digital photographs of the prepared films and the encircled image belongs to the burned sample of TFR65, showing the formation of an intumescent char formation.

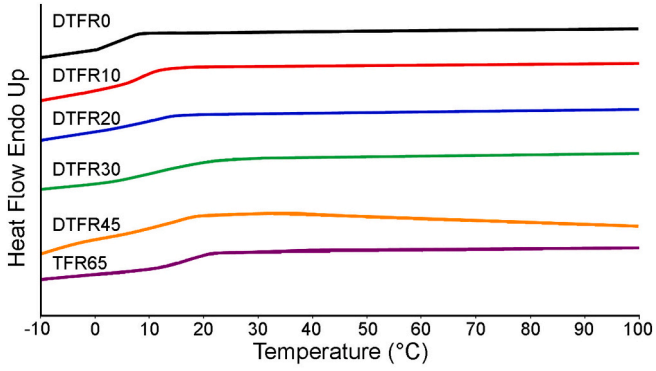

Fig. 8. DSC curves of the thermosets.

and the triazole rings.

In terms of thermal properties, we also determined the T_g values of the thermosets (Table 2). The DSC curves are shown in Fig. 8. The T_g of the base formulation was found as 4.4 °C. The T_g of the crosslinked networks composed of DATP and pentaerythritol tetrakis(3-mercaptobutyrate), was previously measured and determined as ~5 °C [34]. Thus, our result is in good accordance with the literature. The increase in the DTDAE amount in the formulations led to an increment of the T_g values. When DAP was replaced with DTDAE, the T_g was raised to 16 °C. With the bulky DOPO unit in the networks as well as the additional molecular interactions due to the polar -P=O and triazole groups, the mobility of the polymer chains was slightly restricted, thus the T_gs increased.

The escalated T_g values indicate that the stiffness of the thermosets was also increased. In such a case, generally, an increase in the modulus of the materials is expected. However, with our crosslinked materials, despite the increased T_g values, a decreasing trend was observed for the modulus values. Thus, according to the DSC and mechanical test results, for the thermosets prepared in this work, we can conclude that the rigid bulky side groups are much more effective in determining the glass transition temperatures rather than the crosslinking density, whereas

the extent of curing was competent for controlling the mechanical properties as noted above.

4. Conclusions

In this work, we successfully demonstrated a metal-free click route for the synthesis of a novel liquid flame retardant monomer and used it for the synthesis of the thermosets via TEP. The main conclusions are as follows:

a) Considering that DOPO-based flame retardants which are generally known in the literature as solid at room temperature and exhibit high melting points, we must note that the newly synthesized reactive monomer; DTDAE, was obtained as a viscous liquid at room temperature. This pleasing feature is advantageous for mixing procedures and for the elimination of solvents.
b) All thermosets prepared with DTDAE exhibited a high degree of curing with sufficient gel content values.
c) The incorporation of DTDAE into the formulations enhanced both the thermal stability and the flame retardancy of the photocrosslinked films. When the DTDAE content was at its highest level, the char yield was increased over two-fold concerning the DTDAE-free formulation, and the LOI value was determined as 27.8%. According to the UL-94 test, TFR65 is classified as a V-0 rating.

The scope of metal-free click reactions which bring new horizons to material designs is ever-expanding. There is a great potential in metal-free click reactions yet to be discovered. They not only offer new perspectives but also instigate sustainable solutions. We believe that these approaches will pioneer the generation of novel flame retardant monomers and agents to be used in industrial applications. The use of such approaches in polymers such as polyurethane foams or epoxy will be considered in future studies.

CRediT authorship contribution statement

Gokhan Sagdic: Investigation **Emrah Çakmakçı:** Investigation, Conceptualization, Writing - Original Draft **Ozgun Daglar:** Writing - Original Draft **Ufuk Saim Gunay:** Conceptualization, Reviewing and Editing, Supervision **Gurkan Hizal:** Reviewing and Editing **Umit Tunca:** Reviewing and Editing **Hakan Durmaz:** Conceptualization, Methodology, Reviewing and Editing.

Declaration of competing interest

The authors declare that they have no known competing financial interests or personal relationships that could have appeared to influence the work reported in this paper.

Appendix A. Supplementary data

Supplementary data to this article can be found online at https://doi.org/10.1016/j.porgcoat.2022.106825.

References

[1] https://www.nfpa.org/~/media/fd0144a044c84fc5baf90c05c04890b7.ashx.
[2] C.E. Hoyle, T.Y. Lee, T. Roper, Thiol–enes: chemistry of the past with promise for the future, J. Polym. Sci. A Polym. Chem. 42 (21) (2004) 5301–5338.
[3] O. Okay, C.N. Bowman, Kinetic modeling of thiol-ene reactions with both step and chain growth aspects, Macromol. Theory Simul. 14 (4) (2005) 267–277.
[4] A.B. Lowe, Thiol-ene "click" reactions and recent applications in polymer and materials synthesis, Polym. Chem. 1 (1) (2010) 17–36.
[5] N.B. Cramer, C.N. Bowman, Thiol-ene and thiol-yne chemistry in ideal network synthesis, in: Thiol-X Chemistries in Polymer and Materials Science, 2013, pp. 1–27.
[6] V. Fındık, I. Degirmenci, Ş. Çatak, V. Aviyente, Theoretical investigation of thiol-ene click reactions: a DFT perspective, Eur. Polym. J. 110 (2019) 211–220.
[7] V. Fındık, B.T. Varinca, I. Degirmenci, S. Sag Erdem, Insight into the thiol-yne kinetics via a computational approach, J. Phys. Chem. A 125 (17) (2021) 3556–3568.
[8] O.A. Urucu, E.D. Aracier, E. Çakmakçi, Allylimidazole containing OSTE based photocured materials for selective and efficient removal of gold from aqueous media, Microchem. J. 146 (2019) 997–1003.
[9] N.B. Cramer, C.N. Bowman, Thiol–ene chemistry, in: W.R. Algar, P.E. Dawson, I. L. Medintz (Eds.), Chemoselective and Bioorthogonal Ligation Reactions, 2017, https://doi.org/10.1002/9783527683451.ch5.
[10] B. Oktay, E. Çakmakçi, DOPO tethered diels Alder clickable reactive silica nanoparticles for bismaleimide containing flame retardant thiol-ene nanocomposite coatings, Polymer 131 (2017) 132–142.
[11] E. Çakmakçı, Y. Mülazim, M.V. Kahraman, N.K. Apohan, Preparation and characterization of boron containing thiol–ene photocured hybrid coatings, Prog. Org. Coat. 75 (1–2) (2012) 28–32.
[12] Emrah Cakmakci, M.V. Kahraman, Boron/Phosphorus-containing flame-retardant photocurable coatings, Photocured Mater. (2015) 150–187.
[13] T. Liu, L. Sun, R. Ou, Q. Fan, L. Li, C. Guo, Q. Wang, Flame retardant eugenol-based thiol-ene polymer networks with high mechanical strength and transparency, Chem. Eng. J. 368 (2019) 359–368.
[14] O. Daglar, E. Çakmakçi, U.S. Gunay, G. Hizal, U. Tunca, H. Durmaz, Acetylene dicarboxylic acid diallyl ester: a versatile monomer for thiol-ene photocured networks, Macromol. Mater. Eng. 2100427 (2021).
[15] M. Cetin, C. Esen, O. Daglar, S. Luleburgaz, G. Hizal, H. Durmaz, U. Tunca, 1, 3-dipolar and diels-Alder cycloaddition reactions on polyester backbones possessing internal electron-deficient alkyne moieties, Polym. Chem. 7 (46) (2016) 7094–7100.
[16] S. Luleburgaz, G. Hizal, H. Durmaz, U. Tunca, Modification of electron deficient polyester via Huisgen/Passerini sequence, Polymer 127 (2017) 45–51.
[17] U.S. Gunay, M. Cetin, O. Daglar, G. Hizal, U. Tunca, H. Durmaz, Ultrafast and efficient aza-and thiol-Michael reactions on a polyester scaffold with internal electron deficient triple bonds, Polym. Chem. 9 (22) (2018) 3037–3054.
[18] E. Baysak, U.S. Gunay, O. Daglar, H. Durmaz, Synthesis and post-polymerization modification of polyester containing pendant thiolactone units, Eur. Polym. J. 112 (2019) 241–247.
[19] O. Daglar, U.S. Gunay, G. Hizal, U. Tunca, H. Durmaz, Extremely rapid polythioether synthesis in the presence of TBD, Macromolecules 52 (9) (2019) 3558–3572.
[20] O. Daglar, E. Çakmakçı, G. Hizal, U. Tunca, H. Durmaz, Extremely fast synthesis of polythioether based phase change materials (PCMs) for thermal energy storage, Eur. Polym. J. 130 (2020), 109681.
[21] O. Daglar, E. Cakmakci, U.S. Gunay, G. Hizal, U. Tunca, H. Durmaz, A straightforward method for fluorinated polythioether synthesis, Macromolecules 53 (8) (2020) 2965–2975.
[22] O. Daglar, B. Gungor, G. Guric, U.S. Gunay, G. Hizal, U. Tunca, H. Durmaz, Rapid hyperbranched polythioether synthesis through thiol-Michael addition reaction, J. Polym. Sci. 58 (6) (2020) 824–830.
[23] O. Daglar, B. Alkan, U.S. Gunay, G. Hizal, U. Tunca, H. Durmaz, Ultrafast synthesis of phosphorus-containing polythioethers in the presence of TBD, Eur. Polym. J. 110931 (2021).
[24] O. Daglar, E. Çakmakçi, U.S. Gunay, G. Hizal, U. Tunca, H. Durmaz, All in one: the preparation of polyester/silica hybrid nanocomposites via three different metal-free click reactions, Eur. Polym. J. 154 (2021), 110532.
[25] G. Sagdic, O. Daglar, U.S. Gunay, E. Cakmakci, G. Hizal, U. Tunca, H. Durmaz, Practical phosphorylation of polymers: an easy access to fully alcohol soluble synthetically and industrially important polymers, Polym. Chem. 12 (31) (2021) 4478–4487.
[26] R. Sonnier, L. Ferry, J.M. Lopez-Cuesta, in: Flame Retardancy of Phosphorus-Containing Polymers, The Royal Society of Chemistry, Oxford, 2014, pp. 252–270.
[27] Y.F. Ai, L. Xia, F.Q. Pang, Y.L. Xu, H.B. Zhao, R.K. Jian, Mechanically strong and flame-retardant epoxy resins with anti-corrosion performance, Compos. Part B 193 (2020), 108019.
[28] Y.F. Ai, F.Q. Pang, Y.L. Xu, R.K. Jian, Multifunctional phosphorus-containing triazolyl amine toward self-intumescent flame-retardant and mechanically strong epoxy resin with high transparency, Ind. Eng. Chem. Res. 59 (26) (2020) 11918–11929.
[29] R.K. Jian, F.Q. Pang, Y.C. Lin, W.B. Bai, Facile construction of lamellar-like phosphorus-based triazole-zinc complex for high-performance epoxy resins, J. Colloid Interface Sci. 609 (2022) 513–522.
[30] Y.F. Ai, X.D. Liu, W.B. Bai, Y.C. Lin, R.R. Xie, R.K. Jian, From herbicide to flame retardant: the lamellar-like phosphorus-bridged amitrole toward high fire safety epoxy resin with light smoke and low toxicity, Chemosphere 291 (2022), 132704.
[31] S.S. Le Corre, M. Berchel, H. Couthon-Gourvès, J.P. Haelters, P.A. Jaffrès, Atherton-Todd reaction: mechanism, scope and applications, Beilstein J. Org. Chem. 10 (1) (2014) 1166–1196.
[32] S. Wagner, M. Rakotomalala, Y. Bykov, O. Walter, M. Döring, Synthesis of new organophosphorus compounds using the Atherton–Todd reaction as a versatile tool, Heteroat. Chem. 23 (2) (2012) 216–222.
[33] M. Hamidov, E. Çakmakçi, M.V. Kahraman, Autocatalytic reactive flame retardants for rigid polyurethane foams, Mater. Chem. Phys. 267 (2021), 124636.
[34] O. Llorente, A. Agirre, I. Calvo, M. Olaso, R. Tomovska, H. Sardon, Exploring the advantages of oxygen-tolerant thiol-ene polymerization over conventional acrylate free radical photopolymerization processes for pressure-sensitive adhesives, Polym. J. (2021) 1–10.
[35] S. Mongkhontreerat, K. Öberg, L. Erixon, P. Löwenhielm, A. Hult, M. Malkoch, UV initiated thiol–ene chemistry: a facile and modular synthetic methodology for the

construction of functional 3D networks with tunable properties, J. Mater. Chem. A 1 (44) (2013) 13732–13737.
[36] Y. Chen, L. Li, L. Qian, The pyrolysis behaviors of phosphorus-containing organosilicon compound modified ammonium polyphosphate with different phosphorus-containing groups, and their different flame-retardant mechanisms in polyurethane foam, RSC Adv. 8 (48) (2018) 27470–27480.
[37] H. Ma, L. Tong, Z. Xu, Z. Fang, Y. Jin, F. Lu, A novel intumescent flame retardant: synthesis and application in ABS copolymer, Polym. Degrad. Stab. 92 (4) (2007) 720–726.
[38] P. Zheng, R. Wang, D. Wang, X. Peng, Y. Zhao, Q. Liu, A phosphorus-containing hyperbranched phthalocyanine flame retardant for epoxy resins, Sci. Rep. 11 (1) (2021) 1–10.
[39] B. Schartel, Phosphorus-based flame retardancy mechanisms—old hat or a starting point for future development? Materials 3 (10) (2010) 4710–4745.